Acceleration of the Hurricane Beta Drift by Shear Strain Rate of an Environmental Flow*

XIAOFAN LI AND BIN WANG

Department of Meteorology, School of Ocean and Earth Science and Technology, University of Hawaii at Manoa, Honolulu, Hawaii

(Manuscript received 7 November 1994, in final form 21 July 1995)

ABSTRACT

An energetics analysis is presented to reveal the mechanisms by which the environmental flows affect hurricane beta-gyre intensity and beta-drift speed. The two-dimensional environmental flow examined in this study varies in both zonal and meridional directions with a constant shear.

It is found that a positive (negative) shear strain rate of the environmental flow accelerates (decelerates) beta drift. The horizontal shear of the environmental flow contains an axially symmetric component that is associated with vertical vorticity and an azimuthal wavenumber two component that is associated with shear strain rate. It is the latter that interacts with the beta gyres, determining the energy conversion between the environmental flow and beta gyres. A positive shear strain rate is required for transfering kinetic energy from the environmental flow to the beta gyres. As a result, the positive shear strain rate enhances the beta gyres and associated steering flow that, in turn, accelerates the beta drift.

1. Introduction

The presence of an environmental flow affects hurricane motion not only by advecting axially symmetric vorticity (steering) but also by changing axially asymmetric beta gyres. The beta gyres result from interactions between the symmetric circulation and the gradients of planetary vorticity (the beta effect) or environmental relative vorticity (e.g., Holland 1983). The circulation associated with the beta gyres advects symmetric vorticity and induces a propagation component (beta drift). The beta drift often represents a deviation from the steering. It is thus of fundamental importance to understand how the presence of a horizontally varying environmental flow influences the beta drift of tropical cyclones.

Previous studies of the effects of environmental flow on hurricane motion have focused on a special environmental flow: zonal flows with meridional shears (e.g., Sasaki 1955; Kasahara 1957; DeMaria 1985), partially because the environmental relative vorticity gradient associated with zonal flows is able to enhance or offset the beta effect. It was found, however, that even without a relative vorticity gradient a zonal flow with a constant anticyclonic (cyclonic) shear can also accelerate (decelerate) beta drift (Ulrich and Smith 1991; Smith 1991) by enhancing (weakening) the beta gyres (Williams and Chan 1994).

Wang and Li (1995, hereafter WL95) developed an energetics theory to explain the physical mechanisms by which a *zonal* flow affects the development of the beta gyres and beta drift. They showed that a zonal flow with an anticyclonic meridional shear feeds kinetic energy to the beta gyres, enhancing the gyre-induced steering flow and accelerating the beta drift. In contrast, a zonal flow with a cyclonic meridional shear extracts energy from the beta gyres and slows down the drift.

The mean tropical flows surrounding a tropical cyclone are not purely zonal and often contain a substantial meridional component. For instance, the vertically averaged winds between 300 and 850 hPa, derived from the European Centre for Medium-Range Weather Forecasts analyses for the period of 10–17 July 1987 (Fig. 1), show that the mean flow consists of a subtropical ridge around 28°N, a monsoon trough to its south, and a westerly trough to its north. The maximum easterly wind along the line AB (Fig. 1) and the maximum northerly wind along the line CD have the same order of magnitude. It is, therefore, necessary to examine influences on beta drift of a more general environmental flow that has both zonal and meridional components.

Since the mean divergent wind is negligibly small compared to the rotational wind, we may approxi-

* School of Ocean and Earth Science and Technology Contribution Number 3956.

Corresponding author address: Prof. Bin Wang, School of Ocean and Earth Science and Technology, University of Hawaii, 2525 Correa Road, Honolulu, HI 96822.

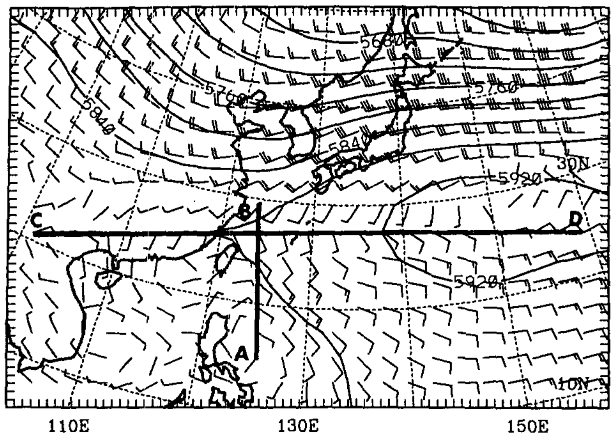

FIG. 1. Vertical mean wind and geopotential height (contour) field calculated by averaging 300, 400, 500, 700 and 850 hPa data for the period of 10–27 July 1987. The data used are from the analyses made by the European Centre for Medium-Range Weather Forecasts. Wind with full barb represents 5 m s^{-1}. The interval of geopotential height is 40 m.

mately express a general mean environmental flow ($\mathbf{U}_e$) in Cartesian coordinates by

$$\mathbf{U}_e = \mathbf{i}U(y) + \mathbf{j}V(x). \tag{1.1}$$

Here, U and V are zonal and meridional components of the environmental flow; **i** and **j** are unit vectors in zonal (x-) and meridional (y-) directions, respectively. Taking a Taylor series expansion for the zonal and meridional winds around an arbitrary point (x_0, y_0), a large-scale total environmental flow can be approximated by a sum of a uniform ($\mathbf{U}_0$) and a linear ($\mathbf{U}_l$) component; that is,

$$\mathbf{U}_e = \mathbf{U}_0 + \mathbf{U}_l, \tag{1.2}$$

where

$$\mathbf{U}_0 = U_0\mathbf{i} + V_0\mathbf{j}, \tag{1.3}$$

$$\mathbf{U}_l(x, y) = U_y(y - y_0)\mathbf{i} + V_x(x - x_0)\mathbf{j}. \tag{1.4}$$

The environmental flow $\mathbf{U}_l$ can represent a variety of environmental flow patterns in the mid to lower troposphere. Figure 2 illustrates such examples. A zonally elongated subtropical anticyclone (Fig. 2a) can be described by a $\mathbf{U}_l$ with $U_y > 0$, $V_x < 0$, and $U_y/V_x = -3$. Similarly, a zonally elongated monsoon depression (Fig. 2b) is described by a $\mathbf{U}_l$ with $U_y < 0$, $V_x > 0$, and $U_y/V_x = -3$. When U_y and V_x are both positive, $\mathbf{U}_l$ represents a saddle flow field. Figures 2c and 2d show two saddle wind fields with $U_y/V_x = 3$ and $U_y/V_x = 1/3$, respectively.

The purpose of the present study is to investigate the effects of a more general environmental flow, which has both zonal and meridional components, on the intensity of the beta gyres and the drift speed, using the approach of the energetics analysis developed in our previous study (WL95).

2. Kinetic energy equations

To investigate the beta drift of a cyclone in horizontally varying barotropic environmental flows, we used a shallow-water model. The model was described in detail in WL95. When the environmental flows are steady solutions of the model equations, their evolution caused by interaction with embedded cyclone is negligibly small and does not affect the cyclone propagation (WL95). For this reason we fix the environmental flows during the time integrations so that the effects of a specified environmental flow on the cyclone propagation can be identified. Since the beta drift depends on the initial structure of a tropical cyclone in a quiescent environment (e.g., Adem 1956; DeMaria 1985; Chan and Williams 1987; Fiorino and Elsberry 1989; Wang and Li 1992; Li and Wang 1994), in order to focus on environmental flow effect, we use the same initial cyclone in all experiments. The azimuthal velocity profile of the initial cyclone is given in Fig. 3.

The total flow **U** consists of an environmental flow $\mathbf{U}_e$ and a cyclone circulation. The cyclone circulation is further decomposed into three components: an axially symmetric circulation $\mathbf{U}_s$, a pair of beta gyres $\mathbf{U}_g$ (azimuthal wavenumber one asymmetric flow), and a

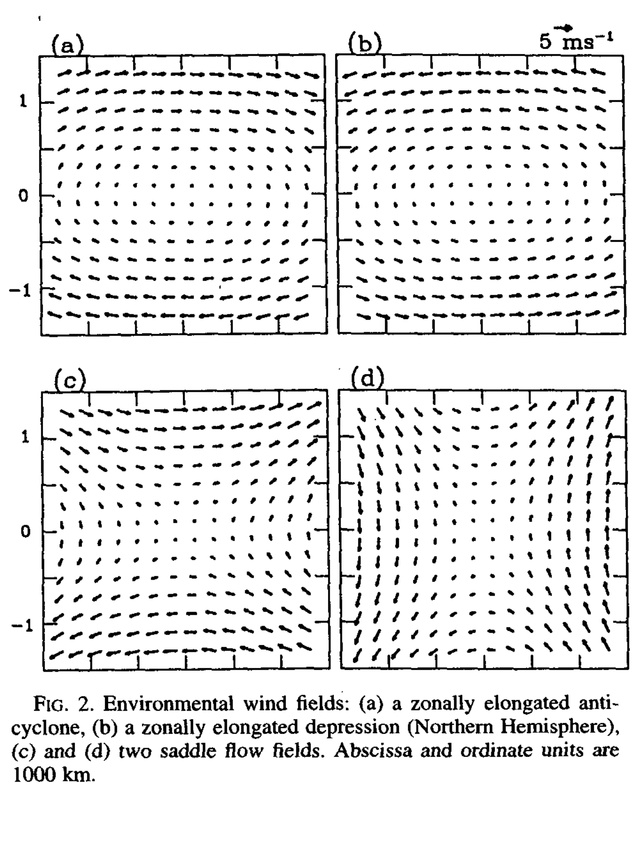

FIG. 2. Environmental wind fields: (a) a zonally elongated anticyclone, (b) a zonally elongated depression (Northern Hemisphere), (c) and (d) two saddle flow fields. Abscissa and ordinate units are 1000 km.

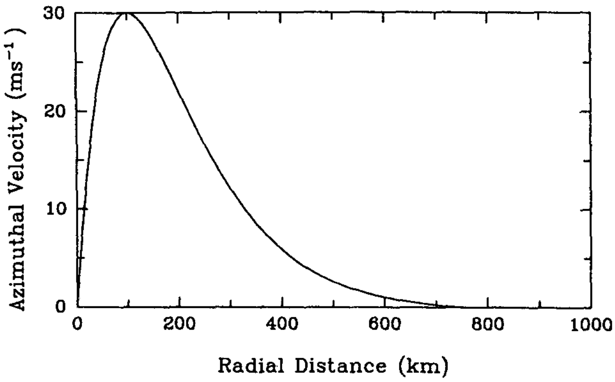

FIG. 3. Azimuthal wind profile of the initial symmetric tropical cyclone used in the model.

residual asymmetric flow $\mathbf{U}_{res}$. The drift speed is determined by the asymmetric flow associated with the beta gyres in the vicinity of the cyclone center (Fiorino and Elsberry 1989). The intensity of the beta gyres can be measured by the amount of kinetic energy K_g. To examine the energy source for the gyre development in an environmental flow, a set of kinetic energy equations for the cyclone circulation was derived in WL95:

$$\frac{\partial K_s}{\partial t} = F_s - (K_s, K_g) - (K_s, K_{res}) + (K_e, K_s), \quad (2.1a)$$

$$\frac{\partial K_g}{\partial t} = F_g + (K_s, K_g) + (K_{res}, K_g) + (K_e, K_g), \quad (2.1b)$$

$$\frac{\partial K_{res}}{\partial t} = F_{res} + (K_s, K_{res}) - (K_{res}, K_g) + (K_e, K_{res}), \quad (2.1c)$$

where K denotes a domain-integrated kinetic energy and F is the outward energy flux across the boundary of integration domain; subscripts e, s, g, and res represent environmental flow and the components of symmetric circulation, gyres, and the residual, respectively; and the notation (A, B) means a kinetic energy conversion from A to B. The detailed derivation of (2.1) and definitions of kinetic energy, energy conversion, and energy flux terms were presented in WL95. Here, we list only the two most important kinetic energy generation equations for the beta gyres. One is the conversion from environmental flow to the beta gyres (K_e, K_g), and the other is the conversion from symmetric circulation to the beta gyres (K_s, K_g). In Cartesian coordinates they are, respectively,

$$(K_e, K_g) = -\langle[(\mathbf{U}_s + \mathbf{U}_g + \mathbf{U}_{res})\cdot\nabla\mathbf{U}_e]\cdot\mathbf{U}_g\rangle, \quad (2.2a)$$

$$(K_s, K_g) = -\langle(\mathbf{U}\cdot\nabla\mathbf{U}_s)\cdot\mathbf{U}_g\rangle + \langle f\mathbf{k}\cdot(\mathbf{U}_g \times \mathbf{U}_s)\rangle, \quad (2.2b)$$

where the angular bracket

$$\langle(\ \ )\rangle = \iint_S (\ \ )dS = \iint_{A(t)} (\ \ )dA = \int_0^R rdr \int_0^{2\pi} (\ \ )d\lambda \quad (2.3)$$

represents an integration over the model domain S. Because of the circular nature of the cyclonic circulation, the integration over the model domain (S) can be evaluated by an integration over a circular domain $A(t)$, whose center is collocated with the center of the moving cyclone and whose radius is sufficiently large. For convenience of analysis the integration is then carried out in the moving system of cylindrical coordinates. For instance, the cylindrical coordinate form of (2.2a) (WL95) is

$$(K_e, K_g) = -\langle[(\mathbf{V}_s + \mathbf{V}_g + \mathbf{V}_{res})\cdot\nabla\mathbf{V}_e]\cdot\mathbf{V}_g\rangle - \langle(\Omega_s + \Omega_g + \Omega_{res})\mathbf{k}\cdot(\mathbf{V}_e \times \mathbf{V}_s)\rangle, \quad (2.4)$$

where $\mathbf{V}$ is the wind vector in cylindrical coordinates, $\Omega = v_\lambda/r$, v_λ is the azimuthal wind component, and $\mathbf{k}$ is a vertical unit vector. Equation (2.4) will be used to diagnose the energy conversion from environmental flow to the beta gyres.

3. Dependence of the drift speed on the environmental shear strain rate

Numerical experiments were performed to assess effects of different types of linear environmental flows, $\mathbf{U}_l(x, y)$, on beta drift. A detailed description of the model was presented in Li and Wang (1994). The model domain covers an area of 6000 km × 6000 km with a square mesh of 40 km. A nine-point smoother was used in the model computation. Time integrations were all carried out for 72 h. The displacement of the cyclone consists of a steering and a beta-drift component. To focus on the latter, the steering component was removed following Williams and Chan (1994). The resultant track is referred to as a beta-drift track.

The beta drift in a zonal flow with an anticyclonic shear ($U_y > 0$, case L_1) is faster, whereas in a zonal flow with a cyclonic shear ($U_y < 0$, case L_2) it is slower than the beta drift in a quiescent environment (case L_0) (Fig. 4). At first glance, this appears to suggest a link between environmental relative vorticity and the beta drift; that is, a negative (positive) environmental relative vorticity accelerates (decelerates) beta drift.

To test the validity of the above speculation, we designed another pair of experiments in which the linear environmental flows are meridional, but one has an anticyclonic shear ($V_x < 0$, case L_3), and the other has a cyclonic shear ($V_x > 0$, case L_4). The magnitudes of the shears in all four cases (L_1, L_2, L_3, and L_4) are identical (Table 1). It was found that the mean beta-

TABLE 1. A summary of characteristic parameters of the environmental flows in series of experiments. Here, f_0 is the Coriolis parameter at 20°N. The definitions of relative vorticity (ζ) and shear strain rate (ϵ) are given in (3.1), and U_y and V_x are defined by meridional variation of zonal flow and zonal variation of meridional flow, respectively.

Case	U_y	V_x	ζ	ϵ
L_0	0.0	0.0	0.0	0.0
L_1	$0.12f_0$	0.0	$-0.12f_0$	$0.12f_0$
L_2	$-0.12f_0$	0.0	$0.12f_0$	$-0.12f_0$
L_3	0.0	$-0.12f_0$	$-0.12f_0$	$-0.12f_0$
L_4	0.0	$0.12f_0$	$0.12f_0$	$0.12f_0$
L_5	$0.06f_0$	$-0.06f_0$	$-0.12f_0$	0.0
L_6	$-0.06f_0$	$0.06f_0$	$0.12f_0$	0.0
L_7	$0.06f_0$	$0.06f_0$	0.0	$0.12f_0$
L_8	$-0.06f_0$	$-0.06f_0$	0.0	$-0.12f_0$

drift speed in case L_3 (where environmental vorticity is negative) is smaller, whereas in case L_4 (where environmental vorticity is positive) it is greater than that in case L_0 (Fig. 4). This disproves the previous statement and indicates that the beta-drift speed does not depend on the relative vorticity of the environmental flow.

We note that a linear environmental flow has not only a constant relative vorticity (ζ) but also a constant shear strain rate (ϵ); these are defined by, respectively,

$$\zeta = V_x - U_y, \tag{3.1a}$$

$$\epsilon = V_x + U_y. \tag{3.1b}$$

Notice that in cases L_1 and L_4, where the beta drift is accelerated, the shear strain rate $\epsilon > 0$, while in cases L_2 and L_3, where the beta drift is decelerated, $\epsilon < 0$. This suggests that a positive (negative) shear strain rate of a linear environmental flow accelerates (decelerates) the beta drift. Examining the beta gyres in each case (Fig. 5) further indicates that the faster beta drift in positive shear strain rate cases is caused by stronger beta gyres. In other words, a positive environmental shear strain rate can enhance the development of the beta gyres, resulting in a faster drift, or vice versa.

In the previous experiments we fixed the initial cyclone structure in order to identify the effects of environmental flows. Does the above conclusion remain valid for cyclones with different structures? To address this issue, we repeated experiments L_1–L_4 for cyclones with deferent structures. In general, the azimuthal wind profile of the initial cyclone shown in Fig. 3 is controlled by three parameters: the maximum wind speed, the radius of the maximum wind, and the radius of the cyclone circulation. By varying these three parameters, a variety of cyclone structures can be acquired. In the absence of the environmental flow the beta-drift speed is proportional to the square root of the mean relative angular momentum (MRAM) (Wang and Li 1992). Therefore, the best way to address the issue is to examine the dependence of beta drift on MRAM in the presence of various shear strain rates. The MRAM of the initial cyclone in the control experiment (L_0) is 1.54 $\times 10^6$ m^2 s^{-1}. We designed two cyclones in the additional experiments A_0 and B_0 that have a smaller and a larger MRAM, respectively (Table 2). For each case, A_0 and B_0, four experiments were performed in which the environmental flows are identical to those used in experiments L_1–L_4. The total drift distances in 72 h are shown in Table 3. It can be seen that the dependence of beta-drift speed on the environmental shear strain rates does not vary with cyclone structure.

To confirm the above conclusion, four more experiments (cases L_5–L_8) were carried out (see Table 1). The environmental flows in cases L_5 and L_6 have either positive (case L_6) or negative (case L_5) relative vorticity, but both have vanishing shear strain rates. The linear flows in cases L_7 and L_8 have either a positive (case L_7) or a negative (case L_8) shear strain rate, but both have vanishing relative vorticity. Cases L_5 and L_6 represent a circular anticyclonic or cyclonic environmental

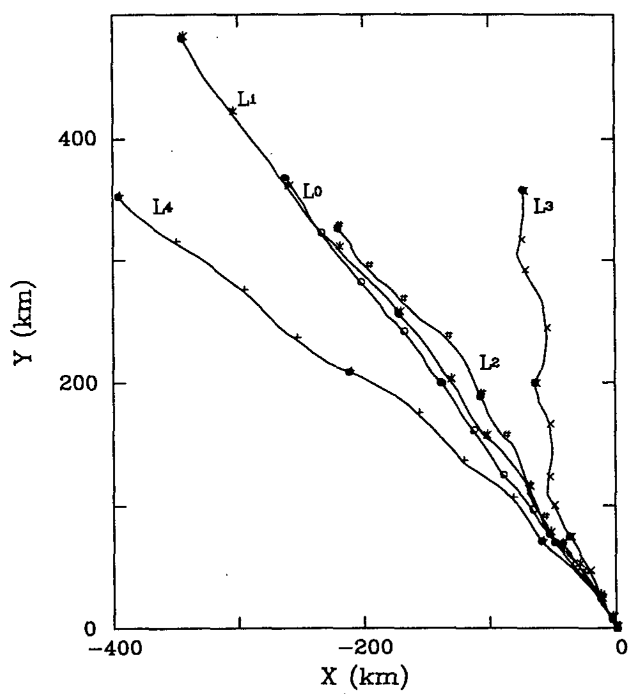

FIG. 4. The beta-drift tracks at 6-h intervals for a resting environment case L_0 (○), linear zonal flow cases L_1 (*) and L_2 (#), and linear meridional flow cases L_3 (×) and L_4 (+). The big closed dots denote the positions of cyclone centers every 24 h. The characteristic parameters of these environmental flows are listed in Table 1. Note that during the first 24 h the beta gyres were gradually generated and the total beta-drift distances do not significantly differ from each other. After this initial adjustment period, the mean beta-drift speed exhibits significant differences.

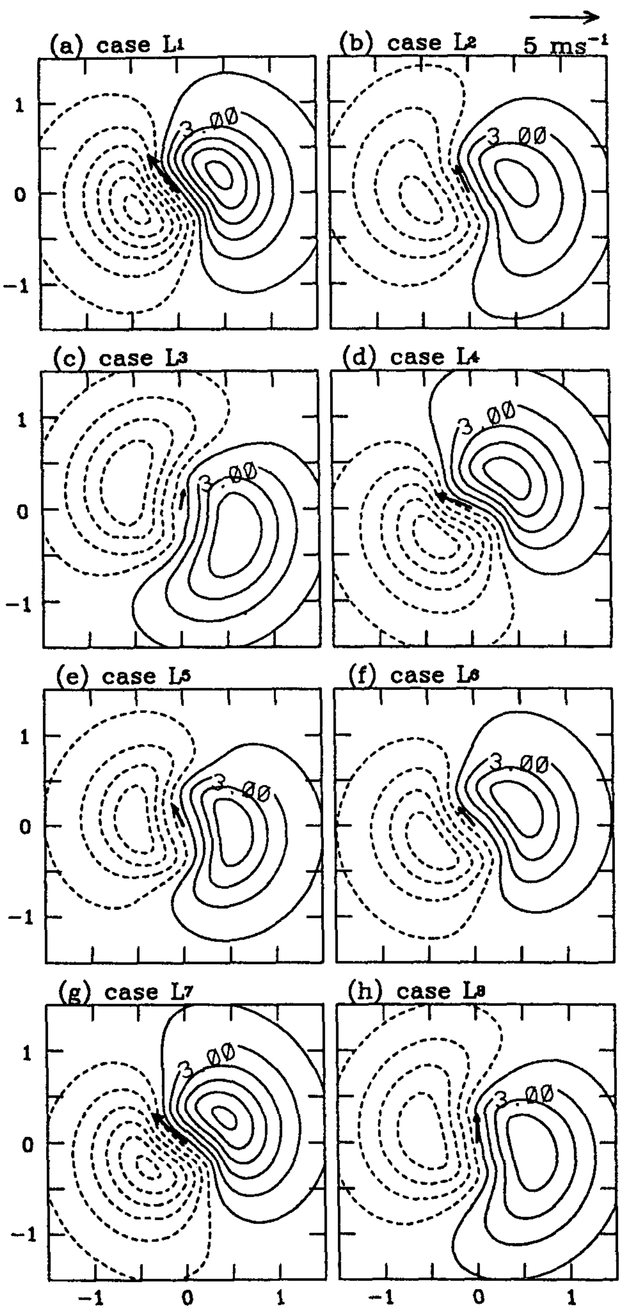

FIG. 5. The streamfunctions of the asymmetric gyres at hour 48 with a contour interval of 2×10^5 m^2 s^{-1} for eight cases listed in Table 1. Arrows at the cyclone center denote beta-drift velocity of the cyclone. Abscissa and ordinate units are 1000 km.

flow field, while cases L_7 and L_8 represent saddle flow patterns similar to those shown in Figs. 2c and 2d.

The 72-h propagation tracks (Fig. 6) show that although the directions between cases L_5 and L_6 are different the total drift distances in both cases are about the same (440 km in case L_5 and 460 km in case L_6).

TABLE 2. Parameters of the azimuthal wind profile for three different initial cyclones: V_m is the maximum wind, r_m is the radius of maximum wind, and R_m is the radius of the cyclone circulation.

Cyclones	V_m (m s^{-1})	r_m (km)	R_m (km)	MRAM (10^6 m^2 s^{-1})
L_0	30	100	750	1.54
A_0	15	100	600	1.02
B_0	30	150	900	3.05

The strengths of the gyres in cases L_5 and L_6 are also similar (Figs. 5e and 5f) to that in a quiescent environment (Fig. 4b in WL95), implying that the environmental flows do not change the beta-gyre intensity because the environmental flows in cases L_5 and L_6 have vanishing shear strain rates. On the other hand, the total distance of propagation track in case L_7 (580 km) is significantly longer than that in case L_8 (400 km) (Fig. 6), because the beta gyres are much stronger in case L_7 than those in case L_8 (Figs. 5g and 5h). This again demonstrates that it is the shear strain rate, rather than the relative vorticity of the environmental flow, that determines the gyres' intensity. It is interesting to observe that the strengths of the gyres in cases L_1, L_4, and L_7 are almost the same (Fig. 5). The environmental flows in these three cases have exactly the same positive shear strain rates (Table 1), so that the rates of the energy conversion (K_s, K_g) are nearly the same. This confirms the conclusion that the shear strain rate of an environmental flow determines the development rate and strength of the beta gyres and the beta-drift speed.

In our experiments we have fixed environmental flow during the integration so that the effects of a specified environmental flow on beta drift can be readily identified. In the first four experiments (L_1–L_4) the specified environmental flows are steady solutions of the model equations, and their evolution and impact on beta drift are negligibly small. In the last four experiments (L_5–L_8), however, the environmental flows have both zonal and meridional shears and are not steady solutions. In these cases the environmental shear strain rates change with time, which may feed back to the beta drift. To check how sensitive the results are to the

TABLE 3. Total beta-drift distances (km) in 72 h for the three cyclones listed in Table 2 in various environmental flows. In the table, $C = 0.587 \times 10^{-5}$ s^{-1}.

		Environmental flows			
Cyclone	Resting	$U_y = C$, $V_x = 0$,	$U_y = -C$, $V_x = 0$,	$U_y = 0$, $V_x = C$,	$U_y = 0$, $V_x = -C$
L_0	453	592	394	530	364
A_0	275	412	243	345	238
B_0	641	937	569	810	517

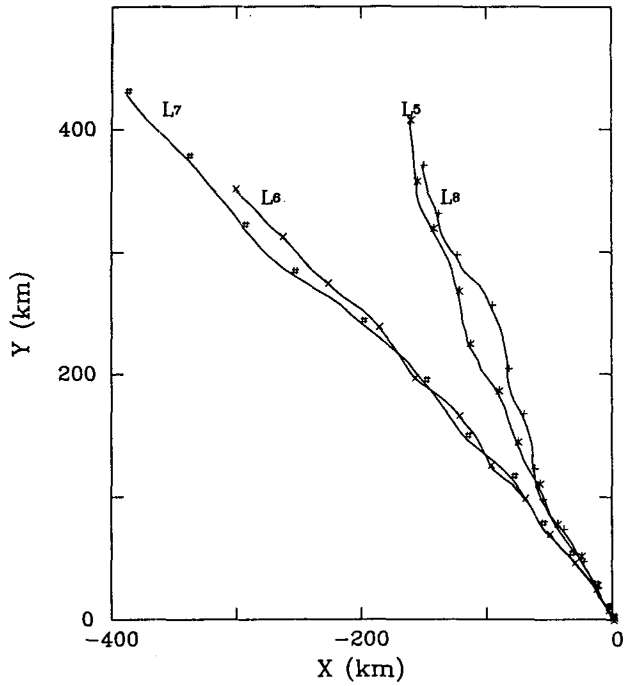

FIG. 6. As in Fig. 4 except for general linear flow cases L_5 (*), L_6 (×), L_7 (#), and L_8 (+).

nonsteadiness of the environmental shearing deformation, we have made comparative experiments with a fully nonlinear model in which the change in environmental flows is determined at each time step. The beta-drift track is obtained by removing the steering effect of the varying environmental flow. The resultant track, however, takes into account the influence due to the interaction between the cyclone circulation and environmental flow. The results show that the feedback due to nonsteadiness of the environmental flows slightly affected beta-drift speed, but the conclusions regarding the dependence of beta-drift speed on shear strain rate remain valid qualitatively. For instance, in the experiments L_7 and L_8 (Table 1) the positive (negative) shear strain rate makes the beta drift faster (slower). After taking into account the effect of nonsteadiness (the corresponding experiments are designated by L_{7n} and L_{8n}, respectively), the beta drift remains significantly faster in L_{7n} (slower in L_{8n}) than that without the shear strain rate, although the acceleration (deceleration) is slightly reduced (Table 4). This indicates that the conclusions remain qualitatively valid when the environmental shearing deformation is nonuniform and varies with time.

4. Effects of the environmental shear strain rate on development of beta gyres

Why does the shear strain rate, instead of the vorticity of an environmental flow, control the gyre strength? An analysis of the kinetic energy source for the gyres may provide useful physical insight. Wang and Li (1995) have shown that the differences in the gyre kinetic energy among different linear zonal flows are primarily due to the conversion term (K_e, K_g). In what follows, we will show that the energy conversion (K_e, K_g) in linear environmental flows depends on the sign and strength of the shear strain rate.

Consider that the cyclone center is located at $x = x_c$, $y = y_c$. The environmental flow (1.4) becomes

$$\mathbf{U}_1(x, y) = iU_y(y_c - y_0) + \mathbf{j}V_x(x_c - x_0) + \mathbf{i}U_y(y - y_c) + \mathbf{j}V_x(x - x_c). \quad (4.1)$$

The first two terms of the right-hand side of (4.1) represent a uniform flow component, which does not affect beta drift. The last two terms of the right-hand side of (4.1), which are the same as (1.4) except that (x_0, y_0) is replaced by (x_c, y_c), denote a linear flow component. Only the horizontal shear of the environmental flow (4.1) plays a role in determining energy conversion (K_e, K_g). In cylindrical coordinates whose origin is located at the cyclone center (x_c, y_c),

$$y - y_c = r\cos\lambda, \quad \text{and} \quad x - x_c = -r\sin\lambda, \quad (4.2)$$

where r is the radial distance and λ the azimuthal angle measured from due north counterclockwise. The radial (V_r) and azimuthal (V_λ) component of horizontal shears of the environmental flow (4.1) are, respectively,

$$V_r = -U_1\sin\lambda + V_1\cos\lambda = -0.5r(V_x + U_y)\sin 2\lambda, \quad (4.3a)$$

$$V_\lambda = -U_1\cos\lambda - V_1\sin\lambda = -0.5r \times (V_x + U_y)\cos 2\lambda + 0.5r(V_x - U_y). \quad (4.3b)$$

In the derivation of (4.3a,b), $U_1 = U_y(y - y_c)$, $V_1 = V_x(x - x_c)$, and (4.2) were used. One should note that a linear environmental flow contains an azimuthal wavenumber two component and an axially symmetric component. Use of (4.3a) and (4.3b) in (2.4) and neglect of the effects of residual asymmetric flow yields

$$(K_e, K_g) = 0.5(V_x + U_y)\langle(V_{rg}^2 - V_{\lambda g}^2)\sin 2\lambda + 2V_{rg}V_{\lambda g}\cos 2\lambda\rangle, \quad (4.4)$$

where V_{rg} and $V_{\lambda g}$ denote the radial and azimuthal wind components of the beta gyres, respectively. Equation (4.4) indicates that the rate of kinetic energy conversion from the environmental shears to the beta gyres is

TABLE 4. Total beta-drift distances (km) in 72 h in the case L_0, L_7, L_8, L_{7n}, and L_{8n}.

Case L_0	Case L_7	Case L_8	Case L_{7n}	Case L_{8n}
453	580	400	540	422

proportional to the shear strain rate of the environmental flows.

The beta gyres shown in Fig. 5 can be primarily described as an azimuthal wavenumber one asymmetric circulation. Assuming that α denotes the azimuthal angle of the anticyclonic gyre center measured counterclockwise from due north, the streamfunction of the beta gyres may be approximately expressed by

$$\psi_g = R_g(r)\cos(\alpha - \lambda), \qquad (4.5)$$

where R_g is the amplitude of the gyres. Substituting (4.5) into (4.4) leads to

$$(K_e, K_g) = 0.5(V_x + U_y)(-\sin 2\alpha)K_g. \qquad (4.6)$$

A cyclone drifts northwestward in the Northern Hemisphere when its anticyclonic gyre is located in the northeast quadrant for which $\sin 2\alpha < 0$. Thus, a positive shear strain rate allows the environmental shears to feed kinetic energy to the gyres, enhancing the steering flow associated with the gyres and accelerating the beta drift. The opposite is true for a negative shear strain rate.

Equation (4.3) indicates that a linear environmental flow contains an axially symmetric component (independent of λ) and a wavenumber two azimuthal component. The former is associated with relative vorticity, whereas the latter is associated with shear strain rate. It is the azimuthal wavenumber two component of the linear environmental flow that interacts with the beta gyres and contributes to the kinetic energy conversion (K_e, K_g).

To interpret the energy conversion process, it is convenient to rewrite (4.4) in Cartesian coordinates. Using the identity $\sin^2 2\lambda + \cos^2 2\lambda = 1$ and transformation

$$V_{rg} = -U_g \sin\lambda + V_g \cos\lambda, \qquad (4.7a)$$

$$V_{\lambda g} = -U_g \cos\lambda - V_g \sin\lambda, \qquad (4.7b)$$

in (4.4) yields

$$(K_e, K_g) = -(V_x + U_y)\langle U_g V_g \rangle, \qquad (4.8)$$

where U_g and V_g are, respectively, zonal and meridional wind components of the beta gyres in Cartesian coordinates. Equation (4.8) indicates that the gyre momentum flux $\langle U_g V_g \rangle$ acting on the shear strain rate of linear environmental flows represents a mechanism of the energy exchange between the linear flow and the gyres.

5. Summary

In this paper we have analyzed the causes for the development of the beta gyres and the effects of the development on beta-drift (propagation) speed for a barotropic cyclone embedded in a horizontally varying environmental flow with constant shear. Such environmental flow can represent a variety of patterns, which resemble some typical environmental flow fields surrounding tropical cyclones. For instance, when the meridional shear of the zonal wind component (U_y) and zonal shear of the meridional wind component (V_x) have opposite signs (thus the shear strain rate vanishes), the flow patterns describe either a subtropical anticyclone or a monsoon depression, depending on the sign of the relative vorticity. When both U_y and V_x have positive signs and the relative vorticity vanishes, the flow pattern represents a saddle field with anticyclonic circulation to the east and west and cyclonic circulation to the south and north, resembling a flow west of a subtropical ridge. In general, the pattern of a linear flow is determined by the ratio of the relative vorticity to shear strain rate of the flow, and the horizontal aspect ratio of the flow pattern depends on the ratio of $|U_y|$ to $|V_x|$.

Recent studies (Ulrich and Smith 1991; Williams and Chan 1994) showed that in a linear zonal flow an anticyclonic (cyclonic) environmental vorticity can accelerate (decelerate) beta drift. We have shown here that in a linear meridional flow an anticyclonic (cyclonic) environmental vorticity decelerates (accelerates) the beta drift. This opposing result indicates that the relative vorticity of an environmental flow does not control beta-drift speed.

We have further demonstrated that the beta-drift speeds depend on the environmental shear strain rates. The horizontal shear of an environmental flow contains an axially symmetric component that is associated with the relative vorticity and an azimuthal wavenumber two component that is associated with the shear strain rate [(3.4)]. The energetics analysis reveals that the azimuthal wavenumber two component of the horizontal shear interacts with the gyres, determining the energy conversion between the environmental flow and the gyres. The energy conversion from the linear environmental flow to the gyres requires a positive shear strain rate of the environmental flow.

The present study focuses only on the factors that determine beta-drift speed. The factors that control the rotation of the beta gyres and the direction of the beta drift will be reported on in an accompanying paper.

Acknowledgments. We wish to thank Mr. X. Chen for data processing and programming assistance. Thanks are also extended to the anonymous reviewers for their relevant comments. This research is supported by the Marine Meteorology Program of the Office of Naval Research under Grant N00014-90-J-1383.

REFERENCES

Adem, J., 1956: A series solution for the barotropic vorticity equation and its application in the study of atmospheric vortices. *Tellus,* **8,** 364–372.

Chan, J. C.-L., and R. T. Williams, 1987: Analytical and numerical studies of the beta-effect in tropical cyclone motion. Part I: Zero mean flow. *J. Atmos. Sci.,* **44,** 1257–1265.

DeMaria, M., 1985: Tropical cyclone motion in a nondivergent barotropic model. *Mon. Wea. Rev.,* **113,** 1199–1209.

Fiorino, M., and R. L. Elsberry, 1989: Some aspects of vortex structure related to tropical cyclone motion. *J. Atmos. Sci.,* **46,** 975–990.

Holland, G. J., 1983: Tropical cyclone motion: Environmental interaction plus a beta effect. *J. Atmos. Sci.,* **40,** 328–342.

Kasahara, A., 1957: The numerical prediction of hurricane movement with the barotropic model. *J. Meteor.,* **14,** 386–402.

Li, X., and B. Wang, 1994: Barotropic dynamics of the beta gyres and beta drift. *J. Atmos. Sci.,* **51,** 746–756.

Sasaki, Y., 1955: Barotropic forecasting for the displacement of a typhoon. *J. Meteor. Soc. Japan,* **32,** 1–8.

Smith, R. K., 1991: An analytic theory of tropical-cyclone motion in a barotropic shear flow. *Quart. J. Roy. Meteor. Soc.,* **117,** 685–714.

Ulrich, W., and R. K. Smith, 1991: A numerical study of tropical cyclone motion using a barotropic model. II: Motion in spatially-varying large-scale flows. *Quart. J. Roy. Meteor. Soc.,* **117,** 107–124.

Wang, B., and X. Li, 1992: The beta drift of three-dimensional vortices: A numerical study. *Mon. Wea. Rev.,* **120,** 579–593.

——, and ——, 1995: Propagation of a tropical cyclone in a meridionally varying zonal flow: An energetics analysis. *J. Atmos. Sci.,* **52,** 1421–1433.

Williams, R. T., and J. C.-L. Chan, 1994: Numerical studies of the beta effect in tropical cyclone motion. Part II: Zonal mean flow effects. *J. Atmos. Sci.,* **51,** 1065–1076.